A Thermodynamic Evaluation of the Cr-Fe-N System

KARIN FRISK

The thermodynamic properties of the Cr-Fe-N system have been analyzed using thermodynamic models describing the Gibbs energy of the individual phases. A two-sublattice model has been used for the interstitial solution phases and a substitutional solution model for the liquid phase. The analysis involves a combination of predictions from recent assessments of the binary sides with computerized optimization of new ternary parameters. A set of parameters describing the Gibbs energy of the body-centered cubic (bcc), face-centered cubic (fcc), ε, CrN, Fe_4N, and liquid phases is given. Using this set of parameters, any type of phase equilibria can be calculated. A number of diagrams are presented comparing the results from the calculations with available experimental data, and the agreement is discussed. Most experimental data are well accounted for. The present study is also compared with a previous evaluation.

I. INTRODUCTION

THERE have been several investigations of the phase relations in the Cr-Fe-N system. Raghavan[1] reviewed the experimental data and proposed a reaction scheme, a liquidus surface, and some isothermal sections. Hertzman and Jarl[2] studied the available experimental data and supplemented this information with some of their own measurements. They analyzed the existing data with the use of thermodynamic models describing the Gibbs energy of each phase. The parameters involved in the models were determined by searching the best fit to experimental data using a computer program. The present work is a reassessment of the Cr-Fe-N system using the same method as Hertzman and Jarl but also including the liquid phase that was not studied previously. Recently, new assessments of the binary systems Cr-Fe, Cr-N, and Fe-N have been presented.[3,4] Therefore, a complete reevaluation was necessary to make the description of solid phases in the ternary Cr-Fe-N system consistent with the binaries. The models for the nitrides have been changed[4] due to new experimental data, and the set of model parameters determined from ternary data is now different. When the reevaluation was performed, new experimental data were taken into account. The most important ones come from a recent investigation by Feichtinger *et al.*[5] on the solubility of N in solid and liquid Cr-Fe alloys under and above 1 atm N_2 pressure. A new selection of experimental data was made, and the data were reanalyzed with the thermodynamic models. With improved computer programming, it is possible to take all experimental data into account simultaneously, whereas Hertzman and Jarl[2] analyzed each temperature separately. An attempt was also made to improve the agreement with experimental data in certain parts of the diagram. Any phase equilibrium or part of a phase diagram can be recalculated from the Gibbs energy functions. The calculations are compared with available experimental data and with the previous assessment.

KARIN FRISK, Doctor, is with the Division of Physical Metallurgy, Royal Institute of Technology, S-100 44 Stockholm, Sweden.
Manuscript submitted September 29, 1989.

II. THERMODYNAMIC MODELS

A. *The Nitrides and the Bcc and Fcc Phases*

The binary Cr-Fe system was previously analyzed by Andersson and Sundman,[3] and their assessment was used in the present work. In this system, ferrite, a body-centered cubic (bcc) solid solution (α), exists as a continuous phase (Figure 1). Austenite, a face-centered cubic (fcc) solid solution (γ), is restricted to the Fe-rich corner. The bcc and fcc phases are described by a two-sublattice model, where it is assumed that Cr and Fe substitute for each other on the first sublattice and N and vacant interstitial sites (denoted Va) on the second. Body-centered cubic and face-centered cubic are thus represented by the model $(Cr, Fe)_1(N, Va)_c$, with $c = 3$ for bcc and $c = 1$ for fcc. The σ phase appears below 1100 K in the Cr-Fe system. Since the solubility of N in σ is not known, this phase was not treated further in the present work.

The binary systems Cr-N and Fe-N were recently assessed[4] and the results used in the present work. In these evaluations, two Cr nitrides, ε (Cr_2N) and CrN, and two Fe nitrides, ε and γ' (Fe_4N), were treated. Firrao *et al.*[6] determined that ε in the Cr-N and Fe-N systems are isomorphic. There is experimental evidence for a solubility of around 10 wt pct Fe in ε-Cr_2N.[7] The ε phase has a hexagonal close-packed (hcp) metal atom arrangement and is approximated with the model $(Cr, Fe)_1(N, Va)_{0.5}$, where $Cr_1Va_{0.5}$ and $Fe_1Va_{0.5}$ are identical to pure Cr and Fe in the hcp state. CrN also has a measurable solubility of Fe, and this phase is described by the model $(Cr, Fe)_1(N, Va)_1$, where Cr_1Va_1 and Fe_1Va_1 represent pure Cr and Fe in the fcc state. The CrN nitride is thus treated as a part of the ternary fcc phase, and it is described with the same set of parameters as austenite. Due to lack of information on Cr in Fe_4N, this phase is treated as a stoichiometric phase.

A thermodynamic model for phases with several sublattices[8] is used to describe the Gibbs energy for the individual phases. For one formula unit of

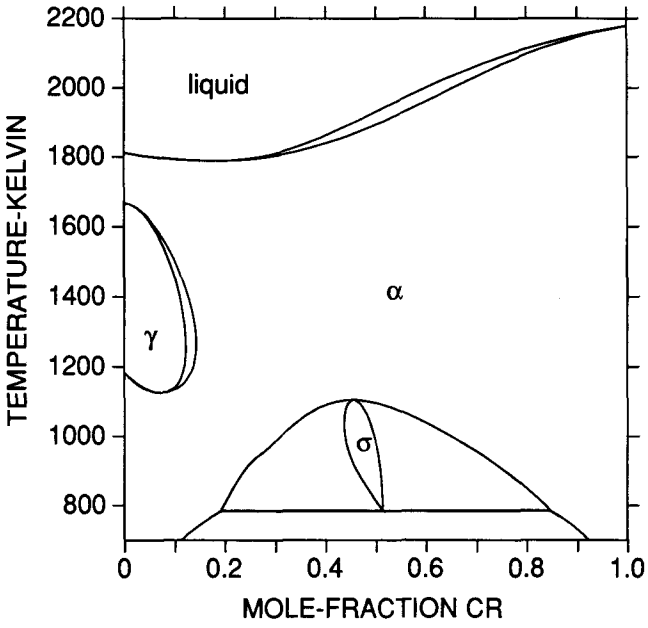

Fig. 1—The calculated Fe-Cr phase diagram.[3]

$(Cr, Fe)_a(N, Va)_c$, this model yields the following expression for the Gibbs energy of each phase:

$$G_m = y_{Cr}y_N{}^\circ G_{Cr:N} + y_{Cr}y_{Va}{}^\circ G_{Cr:Va} + y_{Fe}y_N{}^\circ G_{Fe:N} + y_{Fe}y_{Va}{}^\circ G_{Fe:Va} + RT(a(y_{Cr} \ln y_{Cr} + y_{Fe} \ln y_{Fe}) + c(y_N \ln y_N + y_{Va} \ln y_{Va})) + {}^E G_m + G_m^{mg}$$

The term y_i represents the fraction of component i on the sublattice it occupies and is related to the ordinary mole fractions as

$$y_{Cr} = x_{Cr}/(1 - x_N) \quad \text{and } y_{Cr} + y_{Fe} = 1$$

$$y_N = (a/c)x_N/(1 - x_N) \quad \text{and } y_N + y_{Va} = 1$$

The parameters ${}^\circ G_{M:Va}$ (M is Cr or Fe) represent the Gibbs energy of the pure component M in a hypothetical nonmagnetic state. These parameters were taken from the evaluations by Andersson[9] and Andersson *et al.*[10] (for Cr) and by Fernández Guillermet and Gustafson[11] (for Fe). The parameter ${}^\circ G_{M:N}$ represents the Gibbs energy of a hypothetical state where all interstitial sites are filled with N. These parameters were recently evaluated from data in the binary systems Cr-N and Fe-N.[4] All ${}^\circ G$ parameters are given relative to the enthalpy of the stable states of the elements at 298.15 K and 0.1 MPa, denoted with the superscript SER.

Table I. List of Symbols

Va	vacant interstitial sites
y_i	site fraction of the component i (i represents Cr, Fe, N, or Va)
M	represents the element Cr or Fe
${}^\circ G_{M:Va}$	Gibbs energy of the pure element M in a hypothetical nonmagnetic state
${}^\circ G_{M:N}$	Gibbs energy of a hypothetical state where all interstitial sites are filled with N
${}^\circ G_M^{liquid}$	Gibbs energy of liquid M
H_M^{SER}	enthalpy of the stable state of the element M at 298.15 K and 0.1 MPa
H_N^{SER}	enthalpy of 1/2 mole N_2 gas at 298.15 K and 1 atm (0.1 MPa)
${}^E G_m$	excess Gibbs energy
G_m^{mg}	magnetic contribution to the Gibbs energy
$L_{A,B:C}$	parameter representing the interaction between A and B with C on the second sublattice
β	parameter related to the total magnetic entropy
T_c	critical temperature for magnetic ordering

The term ${}^E G_m$ represents the excess Gibbs energy, and the term G_m^{mg} is a contribution due to magnetic ordering. The excess Gibbs energy is represented by

$${}^E G_m = y_{Cr}y_{Fe}(y_N L_{Cr,Fe:N} + y_{Va}L_{Cr,Fe:Va}) + y_N y_{Va}(y_{Cr}L_{Cr:N,Va} + y_{Fe}L_{Fe:N,Va})$$

The L parameters are interaction parameters. The commas separate elements that interact on the same sublattice, and the colons separate elements on different sublattices. They are composition dependent according to the Redlich-Kister expansion series. The value of $L_{Cr,Fe:Va}$ was taken from the evaluation of the Cr-Fe system by Andersson and Sundman[3] and the parameters $L_{M:N,Va}$ from Reference 4. The parameter $L_{Cr,Fe:N}$ was determined for each phase in the present work. For the evaluation of the fcc phase, a reciprocal parameter was used, and a term $y_{Cr}y_{Fe}y_N y_{Va}L_{Cr,Fe:N,Va}$ was added to the expression for ${}^E G_m$.

The contribution due to magnetic ordering, G_m^{mg}, is described by the model proposed by Hillert and Jarl[12] (Table II). In the present work, it was assumed that the magnetic contribution to the bcc phase is independent of the N content. For the nitrides, it was assumed that there is no magnetic contribution.

In representing the phase diagrams, it is convenient to use a fraction that is independent of the phase, such as the u fractions:

$$u_{Cr} = x_{Cr}/(1 - x_N)$$

$$u_N = x_N/(1 - x_N)$$

The parameters for N_2 gas were given in Reference 4. In the figures and tables where the N activity, a_N, is given, it is equal to $\sqrt{p_{N_2}}$ in atmospheres.

B. *The Liquid Phase*

The liquid phase was treated with a substitutional solution model:

$$G_m = y_{Cr}{}^\circ G_{Cr} + y_{Fe}{}^\circ G_{Fe} + y_N{}^\circ G_N + RT(y_{Cr} \ln y_{Cr} + y_{Fe} \ln y_{Fe} + y_N \ln y_N) + {}^E G_m$$

with

$${}^E G_m = y_{Cr}y_{Fe}L_{Cr,Fe} + y_{Cr}y_N L_{Cr,N} + y_{Fe}y_N L_{Fe,N} + y_{Cr}y_{Fe}y_N L_{Cr,Fe,N}$$

The ${}^\circ G$ terms are taken from References 9 (for Cr), 11 (for Fe), and 4 (for N). The term $L_{Cr,Fe}$ is taken from Reference 9 and the two following L terms from

Table II. List of Parameters Describing the Thermodynamic Parameters of the Cr-Fe-N System*

Bcc

2 sublattices; sites 1:3; constituents Cr, Fe:N, Va

$298.15 < T < 2180.00$

$^{\circ}G^{bcc}_{Cr:Va} - H^{SER}_{Cr} = -8851.93 + 157.48T - 26.908T \ln T + 0.00189435T^2 - 1.47721\ 10^{-6}T^3 + 139{,}250T^{-1}$

$2180.00 < T < 6000.00$

$^{\circ}G^{bcc}_{Cr:Va} - H^{SER}_{Cr} = -34{,}864 + 344.18T - 50T \ln T - 2.88526\ 10^{32}T^{-9}$

$298.15 < T < 1811.00$

$^{\circ}G^{bcc}_{Fe:Va} - 1H^{SER}_{Fe} = +1224.83 + 124.134T - 23.5143T \ln T - 0.00439752T^2 - 5.89269\ 10^{-8}T^3 + 77{,}358.5T^{-1}$

$1811.00 < T < 6000.00$

$^{\circ}G^{bcc}_{Fe:Va} - 1H^{SER}_{Fe} = -25{,}384.451 + 299.31255T - 46T \ln T + 2.2960305\ 10^{31}T^{-9}$

$$^{\circ}G^{bcc}_{Cr:N} = +^{\circ}G^{bcc}_{Cr:Va} + \frac{3}{2}{}^{\circ}G^{gas}_{N_2} + 311{,}870 + 29.12T$$

$$^{\circ}G^{bcc}_{Fe:N} = +\frac{3}{2}{}^{\circ}G^{gas}_{N_2} + {}^{\circ}G^{bcc}_{Fe:Va} + 93{,}562 + 165.07T$$

$^{0}L^{bcc}_{Cr:N,Va} = -200{,}000$

$^{0}L^{bcc}_{Cr,Fe:Va} = +20{,}500 - 9.68T$

$^{**0}L^{bcc}_{Cr,Fe:N} = -799{,}379 + 293T$

$T_c = -311y_{Cr} + 1043y_{Fe} + y_{Cr}y_{Fe}(1650 + 550(y_{Cr} - y_{Fe}))$

$\beta = -0.008y_{Cr} + 2.22y_{Fe} - y_{Cr}y_{Fe}0.85$

Negative values of T_c and β should be divided by -1.

The magnetic contribution to Gibbs energy is described by $G^{mg}_m = RT \ln (\beta + 1)f(\tau)$, $\tau = T/T_c$

$$\text{for } \tau < 1\text{: } f(\tau) = 1 - \left[\frac{79\tau^{-1}}{140p} + \frac{474}{497}\left(\frac{1}{p} - 1\right)\left(\frac{\tau^3}{6} + \frac{\tau^9}{135} + \frac{\tau^{15}}{600}\right)\right]\Big/A$$

$$\text{and for } \tau > 1\text{: } f(\tau) = -\left(\frac{\tau^{-5}}{10} + \frac{\tau^{-15}}{315} + \frac{\tau^{-25}}{1500}\right)\Big/A$$

$$\text{where } A = \left(\frac{518}{1125}\right) + \left(\frac{11{,}692}{15{,}975}\right)\left[\left(\frac{1}{p}\right) - 1\right] \text{ and } p \text{ depends on the structure } p = 0.4 \text{ for bcc.}$$

Fcc (including CrN)

2 sublattices; sites 1:1; constituents Cr, Fe:N, Va

$^{\circ}G^{fcc}_{Cr:Va} = +^{\circ}G^{bcc}_{Cr:Va} + 7284 + 0.163T$

$298.15 < T < 1811.00$

$^{\circ}G^{fcc}_{Fe:Va} = +^{\circ}G^{bcc}_{Fe:Va} - 1462.4 + 8.282T - 1.15T \ln T + 6.4\ 10^{-4}T^2$

$1811.00 < T < 6000.00$

$^{\circ}G^{fcc}_{Fe:Va} - H^{SER}_{Fe} = -27{,}098.266 + 300.25256T - 46T \ln T + 2.78854\ 10^{31}T^{-9}$

$$^{\circ}G^{fcc}_{Cr:N} = +^{\circ}G^{bcc}_{Cr:Va} + \frac{1}{2}{}^{\circ}G^{gas}_{N_2} - 124{,}460 + 142.16T - 8.5T \ln T$$

$$^{\circ}G^{fcc}_{Fe:N} = +^{\circ}G^{bcc}_{Fe:Va} + \frac{1}{2}{}^{\circ}G^{gas}_{N_2} - 37{,}460 + 375.42T - 37.6T \ln T$$

$^{0}L^{fcc}_{Cr:N,Va} = 20{,}000$

$^{0}L^{fcc}_{Fe:N,Va} = -26{,}150$

$^{0}L^{fcc}_{Cr,Fe:Va} = +10{,}833 - 7.477T$

$^{1}L^{fcc}_{Cr,Fe:Va} = 1410$

$^{**0}L^{fcc}_{Cr,Fe:N} = -128{,}930 + 86.49T$

$^{**1}L^{fcc}_{Cr,Fe:N} = +24{,}330$

$^{**0}L^{fcc}_{Cr,Fe:N,Va} = -162{,}516$

Fe_4N

2 sublattices; sites 4:1; constituents Fe:N

Table II Cont. List of Parameters Describing the Thermodynamic Parameters of the Cr-Fe-N System*

$${}^{\circ}G^{Fe_4N}_{Fe:N} = +4{}^{\circ}G^{bcc}_{Fe:Va} + \frac{1}{2}{}^{\circ}G^{gas}_{N_2} - 38{,}744 + 73.52T$$

Hcp (ε)

2 sublattices; sites 1:0.5; constituents Cr, Fe:N, Va

$${}^{\circ}G^{hcp}_{Cr:Va} = +{}^{\circ}G^{bcc}_{Cr:Va} + 4438$$

$298.15 < T < 1811.00$

$${}^{\circ}G^{hcp}_{Fe:Va} - 1H^{SER}_{Fe} = -2480.955 + 136.7255T - 24.6643T \ln T - 0.00375752T^2 - 5.89269\ 10^{-8}T^3 + 77{,}358.5T^{-1}$$

$1811.00 < T < 6000.00$

$${}^{\circ}G^{hcp}_{Fe:Va} - 1H^{SER}_{Fe} = -29{,}341.65 + 304.56206T - 46T \ln T + 2.78853995\ 10^{31}T^{-9}$$

$${}^{\circ}G^{hcp}_{Cr:N} = +{}^{\circ}G^{bcc}_{Cr:Va} + \frac{1}{4}{}^{\circ}G^{gas}_{N_2} - 65{,}760 + 64.69T - 3.93T \ln T$$

$${}^{\circ}G^{hcp}_{Fe:N} = +{}^{\circ}G^{bcc}_{Fe:Va} + \frac{1}{4}{}^{\circ}G^{gas}_{N_2} - 12{,}015 + 37.98T$$

$${}^{0}L^{hcp}_{Cr:N,Va} = +21{,}120 - 10.61T$$

$${}^{1}L^{hcp}_{Cr:N,Va} = -6204$$

$${}^{0}L^{hcp}_{Fe:N,Va} = +10{,}345 - 19.71T$$

$${}^{1}L^{hcp}_{Fe:N,Va} = -11{,}130 + 11.84T$$

$${}^{0}L^{hcp}_{Cr,Fe:Va} = +10{,}833 - 7.477T$$

$$**{}^{0}L^{hcp}_{Cr,Fe:N} = +12{,}826 - 19.48T$$

Liquid

1 sublattice; site 1; constituents Cr, Fe, N

$298.15 < T < 2180.00$

$${}^{\circ}G^{liquid}_{Cr} = +{}^{\circ}G^{bcc}_{Cr:Va} + 24{,}335.93 - 11.42T + 2.37615\ 10^{-21}T^7$$

$2180.00 < T < 6000.00$

$${}^{\circ}G^{liquid}_{Cr} - 1H^{SER}_{Cr} = -16{,}459 + 335.618T - 50T \ln T$$

$298.15 < T < 1811.00$

$${}^{\circ}G^{liquid}_{Fe} = +{}^{\circ}G^{bcc}_{Fe:Va} + 12{,}040.17 - 6.55843T - 3.6751551\ 10^{-21}T^7$$

$1811.00 < T < 6000.00$

$${}^{\circ}G^{liquid}_{Fe} - 1H^{SER}_{Fe} = -10{,}839.7 + 291.302T - 46T \ln T$$

$${}^{\circ}G^{liquid}_{N} = +\frac{1}{2}{}^{\circ}G^{gas}_{N_2} + 29{,}950 + 59.02T$$

$${}^{0}L^{liquid}_{Cr,N} = -161{,}800 - 16.11T$$

$${}^{1}L^{liquid}_{Cr,N} = 65{,}508$$

$${}^{0}L^{liquid}_{Cr,Fe} = -14{,}550 + 6.65T$$

$${}^{0}L^{liquid}_{Fe,N} = -19{,}930 - 12.01T$$

$$**{}^{0}L^{liquid}_{Cr,Fe,N} = -340{,}750 + 187.4T$$

N_2 gas

1 sublattice; site 1; constituent N

$298.15 < T < 950.00$

$$\frac{1}{2}{}^{\circ}G^{gas}_{N_2} - H^{SER}_{N} = -3750.675 - 9.45425T - 12.7819T \ln T - 0.00176686T^2 + 2.680735\ 10^{-9}T^3 - 32374T^{-1}$$

$950.00 < T < 3350.00$

$$\frac{1}{2}{}^{\circ}G^{gas}_{N_2} - H^{SER}_{N} = -7358.85 + 17.2003T - 16.3699T \ln T - 6.5107\ 10^{-4}T^2 + 3.0097\ 10^{-8}T^3 + 563{,}070T^{-1}$$

$3350.00 < T < 6000.00$

$$\frac{1}{2}{}^{\circ}G^{gas}_{N_2} - H^{SER}_{N} = -16{,}392.8 + 50.26T - 20.4695T \ln T + 2.397545\ 10^{-4}T^2 - 8.3331\ 10^{-9}T^3 + 4{,}596{,}375T^{-1}$$

*The parameters evaluated in the present work are denoted by **. Values are given in SI units.

Reference 4. The ternary term was evaluated in the present work.

III. EVALUATION OF MODEL PARAMETERS

In the following section, it is described how a set of experimental data is selected from the available experimental data. Each piece of information was given a weight that is chosen by personal judgment. The weight should reflect the experimental uncertainty and is changed by trial and error during the course of the work. The weighted set of data was analyzed using the thermodynamic models described above. The ternary experimental data that are available permit the evaluation of a number of parameters. This evaluation was done using a computer optimization program.[13] The computer program calculates an optimum value for the undetermined parameters by minimizing the weighted sum of squared deviations between calculated values and experimentally determined values. Different choices of weights and parameters were tried until most of the data were reproduced by the calculations within the expected uncertainty limits. The parameter values obtained in the present work are given in Table II. In the following sections, the parameter evaluation is described in more detail for each phase.

A. *The Bcc Phase*

Schwerdtfeger[14] studied the solubility of N in Cr-Fe alloys with 20 to 99.1 wt pct Cr. The specimens were nitrided in different $N_2 + H_2$ mixtures. The equilibrium N content, at 1473 K and N_2 pressures up to 0.4 atm, was measured. The alloys exposed to the highest partial pressures of N_2 precipitated γ or ε, and the equilibrium pressure for the $\alpha + \gamma$ and the $\alpha + \varepsilon$ regions can thus be estimated. Turkdogan and Ignatowicz[15] studied the N solubility in Cr-Fe alloys with up to 30 pct Cr, both in ferrite and in austenite, at varying partial pressures of N_2. Their results for ferrite are in good agreement with Schwerdtfeger's data, and the results from both studies were used in the optimization. Lebienvenu and Dubois[16] also measured the solubility of N in bcc, in alloys ranging from 2 to 23.6 pct Cr, equilibrated with N_2 gas with up to 0.4 atm pressure, and at temperatures from 1078 to 1358 K. At the highest N_2 pressures, a second phase precipitated, indicating the solubility limit in α. The Lebienvenu and Dubois[16] data for an alloy with 13.6 pct Cr extrapolated to 1 atm are compared with recent measurements by Feichtinger *et al.*[5] in Figure 2. Feichtinger *et al.*[5] measured the solubility of N in ferrite at high temperatures in equilibrium with 1 atm N_2 gas. Figure 2 shows that the data by Feichtinger *et al.* predict a different temperature dependence of the solubility of N in bcc than do the data by Lebienvenu and Dubois. The activity corresponding to the solubility limit of N in α was measured by Lebienvenu and Dubois to be around 0.5 at 1273 K. This is completely outside the α-phase range measured by Hertzman and Jarl[2] at the same temperature. For these reasons, it was decided not to use the experimental data by Lebienvenu and Dubois in the present work. The data by Schwerdtfeger[14] and Turkdogan and Ignatowicz,[15] at 1473 K, were used, and the temperature dependence of $L_{Cr,Fe:N}$ was determined from the data by Feichtinger *et al.*[5] The calculated results are plotted in Figures 2 and 3, together with the selected experimental data described above. There is a good agreement between calculated and experimental values.

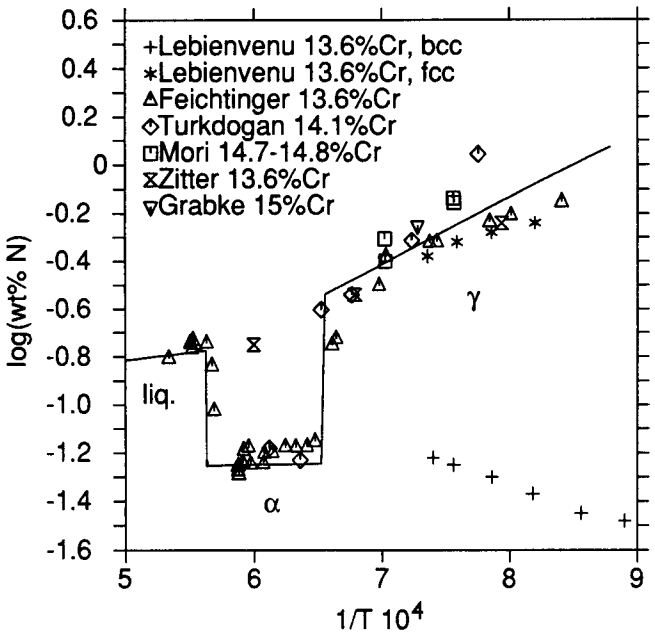

Fig. 2—The calculated solubility of N in an Fe-13.6 pct Cr alloy, in liquid, α and γ in equilibrium with 1 atm N_2 gas, together with experimental data.[5,16–21]

B. *The Fcc Phase*

1. *Experimental data*

For the evaluation of the parameters for the fcc phase, experimental data on activities of N in γ were available. Turkdogan and Ignatowicz[15] measured the solubility in a number of austenitic Cr-Fe alloys at 1473 K in equilibrium with N_2 gas of varying pressures up to a maximum of 1 atm. Recently, Feichtinger *et al.*[5] determined the solubility behavior in γ at higher pressures. A high-pressure furnace was used where a sample could be exposed to a N_2 atmosphere with pressures up to 20 atm. Three alloys with 8.1, 13.6, and 18.4 pct Cr were equilibrated with pressures up to 10 atm at temperatures from 1273 to 1573 K. Feichtinger *et al.* also measured the variation of the solubility of N with temperature in an Fe-13.6 pct Cr alloy in equilibrium with 1 atm N_2 gas. Other authors[17–21] have studied this equilibrium at compositions close to 13.6 pct Cr. The results are in good agreement. Turkdogan and Ignatowicz[19] and Schenck *et al.*[22] studied the solubility in alloys with lower Cr contents as well. All these data were used, weighting the most recent data[5] highest.

Measurements on the $\alpha + \gamma$ equilibrium were also used for the evaluation of the fcc phase parameters. The solubility limit of N in ferrite and in austenite in equilibrium with each other can be estimated from the results of Turkdogan and Ignatowicz.[15] Their measurements show that a lower N_2 pressure is needed to transform a 30 pct Cr alloy from ferrite into austenite than to transform one with only 20 pct Cr. This was confirmed by

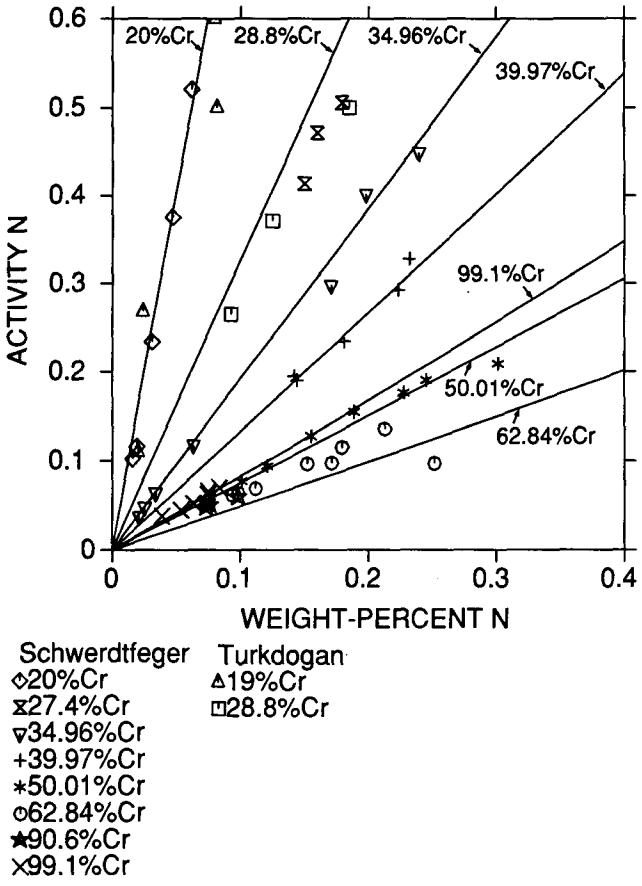

Fig. 3—The calculated solubility of N in α at 1473 K, calculated for a number of Cr contents, compared with experimental data.[14,15]

Jarl and Lindblad,[7] who measured the distribution of Cr between austenite and ferrite at 1473 K in various Cr-Fe alloys at different known partial pressures of nitrogen. The Cr contents in the phases were measured by microprobe. Jarl and Lindblad found that the activity for the two-phase equilibrium increases up to about 25 pct Cr and then decreases. Hertzman and Jarl[2] determined the distribution of Cr between α and γ at 1273 K by microprobe measurement on a sample prepared using a sealed capsule technique. The N activity in the capsule was calculated by Hertzman and Jarl from the analyzed N content in single-phase specimens from the same capsule.

As mentioned in Section II–A, the CrN nitride is described with the fcc phase parameters. Therefore, data on the CrN nitride must be included in the optimization of these parameters. The only experimental data on CrN that were used came from a study by Hertzman and Jarl[2] of the $\gamma + \varepsilon +$ CrN three-phase equilibrium at 1273 K (Table III). They determined the Cr content in the three phases and calculated the N activity of the equilibrium (as described above).

2. *Parameter evaluation*

Austenite and the CrN nitride are separated by a large miscibility gap in the fcc phase. To fit the solubility limit $\gamma/\gamma +$ CrN, this miscibility gap must be adjusted. This was done best by adding a reciprocal parameter, $L_{Cr,Fe:N,Va}$, and fixing its value to get the correct tie lines for the $\gamma +$ CrN equilibria. All binary parameters for the fcc phase were previously determined. It remains to determine the ternary parameter, $L_{Cr,Fe:N}$. To fit the high-pressure data by Feichtinger *et al.*,[5] two terms were introduced through $L_{Cr,Fe:N} = {}^0L_{Cr,Fe:N} + (y_{Cr} - y_{Fe})^1L_{Cr,Fe:N}$ (Table II). A good fit of most of the high-pressure data was obtained, as shown in Figure 4 for 1473 K. The solubility of N at 1 atm N_2 gas is also well described by these parameters, as shown in Figures 2 and 5. The calculated $\alpha + \gamma$ equilibria, together with experimental data, are presented in Tables III and IV, and the equilibria involving the CrN phase are listed in Table III. These results will be discussed in Section IV.

C. *The ε Phase*

1. *Experimental data*

Experimental data on equilibria among α, γ or CrN, and ε were used for the evaluation of the parameters of the ε phase. Jarl and Lindblad[7] measured the distribution of Cr between γ and ε in one sample at 1473 K. The equilibrium N_2 pressure was given as 0.97 atm (Table IV). They also determined the Fe and Cr contents of the three-phase equilibrium among α, γ, and ε at 1473 K, but for this equilibrium, the N_2 pressure was not measured. These data were used in the optimization. Hertzman and Jarl[2] determined the distribution of Cr and Fe among different phases at 1273 K, as described above. They studied the $\alpha + \gamma + \varepsilon$ three-phase equilibrium, as well as the $\gamma + \varepsilon +$ CrN three-phase equilibrium, and analyzed a number of samples in various one- and two-phase regions of the ternary system. A selection of these data, used by Hertzman and Jarl for their own evaluation of the system,[2] was used in the present evaluation. Imai *et al.*[23] investigated a number of isothermal sections between 973 and 1573 K by optical and electron microscopy and X-ray analysis of nitrided and annealed Fe-Cr alloys. They did not determine phase boundaries but only phase compositions of their alloys. Firrao *et al.*[6,24] studied the Fe-rich corner of the isothermal sections at 973 and 840 K by chemical and X-ray analysis of nitrided Fe-Cr alloys.

2. *Parameter evaluation*

The data by Jarl and Lindblad[7] and Hertzman and Jarl[2] from 1273 and 1473 K were used to evaluate a temperature-dependent ternary L parameter for the ε phase (Table II). The calculated results are compared with experimental data in Tables III and IV and will be discussed later. The data from other temperatures were used for a comparison (Section IV).

D. *The Liquid Phase*

1. *Experimental data*

The solubility of N in liquid Cr-Fe alloys in equilibrium with 1 atm N_2 gas has been measured by several investigators. Some of these measurements[25–30] were selected for the present work. Pomarin *et al.*[31] measured the solubility of N in liquid Cr-Fe alloys at 2073, 2173, and 2273 K for alloys with up to 40 pct Cr and N_2 pressures up to 6 atm. Bezobrazov *et al.*[27] measured the solubility of N in liquid Cr-Fe alloys at 1873 K and N_2 pressures from 1 to 50 atm, the alloys ranging from

Table III. Distribution of Chromium among α, γ, ε, and CrN at 1273 K*

Phases	a_N	Ferrite (α) u_{Cr}^{α}	Austenite (γ) u_{Cr}^{γ}	ε (Cr_2N) u_{Cr}^{ε}	CrN u_{Cr}^{CrN}	
$\alpha + \gamma$	0.205,** 0.204†	0.202	0.191	—	—	exp.
	0.189	0.202	0.195	—	—	calc.
$\alpha + \gamma + \varepsilon$	0.205,** 0.204†	0.223	0.223	0.953	—	exp.
	0.191	0.215	0.220	0.956	—	calc.
$\alpha + \varepsilon$	0.205,** 0.204†	0.228	—	0.946	—	exp.
	0.175	0.228	—	0.958	—	calc.
$\alpha + \varepsilon$	0.212,** 0.192†	0.242	—	0.955	—	exp.
	0.161	0.228	—	0.959	—	calc.
$\gamma + \varepsilon$	0.368,** 0.372†	—	0.182	0.944, 0.948	—	exp.
	0.248	—	0.182	0.952	—	calc.
γ + CrN	0.975	—	0.083	—	—	exp.
	0.975	—	0.079	—	1.0	calc.
$\gamma + \varepsilon$ + CrN	0.807,** 0.887†	—	0.140	0.920	0.969	exp.
	0.84	—	0.094	0.922	0.999	calc.

*The values calculated in the present work (noted "calc." in the last column) are compared with experimental data from the work by Hertzman and Jarl[2] (noted "exp." in the last column).

**Calculated by Hertzman and Jarl[2] from the measured N content of single-phase specimens from the same capsule.

†Calculated in the present work from the N content of the single-phase specimens, using the thermodynamic parameters from Table II.

19 to 90 pct Cr. Feichtinger *et al.*[5] measured the N solubility in liquid Cr-Fe alloys with lower Cr content, up to 35 pct Cr, also at 1873 K, in equilibrium with N_2 gas of up to 100 atm. At low Cr contents, the solubility increases linearly with the N_2 pressure, but the deviation from linearity increases as the Cr content and N solubility rise.

2. *Parameter evaluation*

A temperature-dependent ternary parameter was evaluated to account for the experimental data described above. The results are shown in Figures 6 through 8. The solubility at 1 atm N_2 is well reproduced by the present calculation at all temperatures and Cr contents (Figure 6). The data by Pomarin *et al.*[31] are also very well described. The results at 2173 K are shown in Figure 7. Figure 8 shows that the data by Bezobrazov *et al.*[27] and Feichtinger *et al.*[5] are only fitted for Cr contents lower than 35 pct Cr. For higher Cr contents, the fit is good only at low N activities. With the model chosen for the liquid phase, described in Reference 4 for the Cr-N and Fe-N systems, it was not possible to describe these data more accurately. The present calculation predicts that the

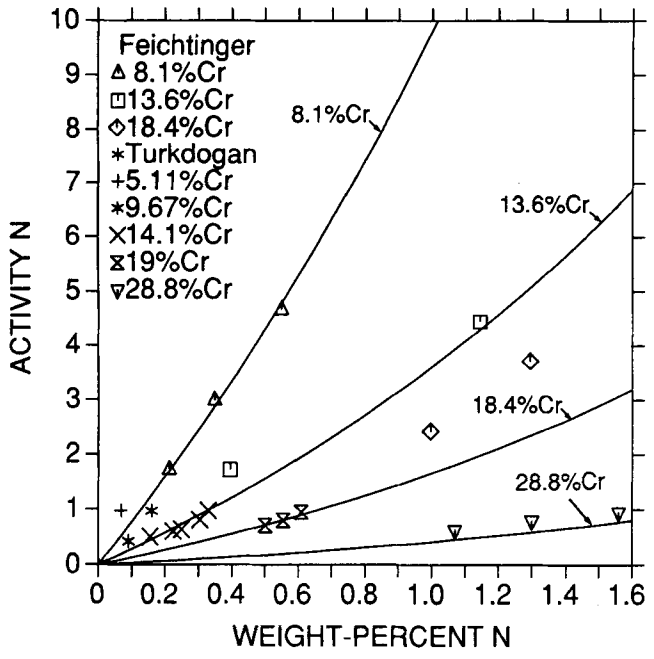

Fig. 4—The calculated solubility of N in γ at 1473 K together with experimental data from Refs. 5 and 15.

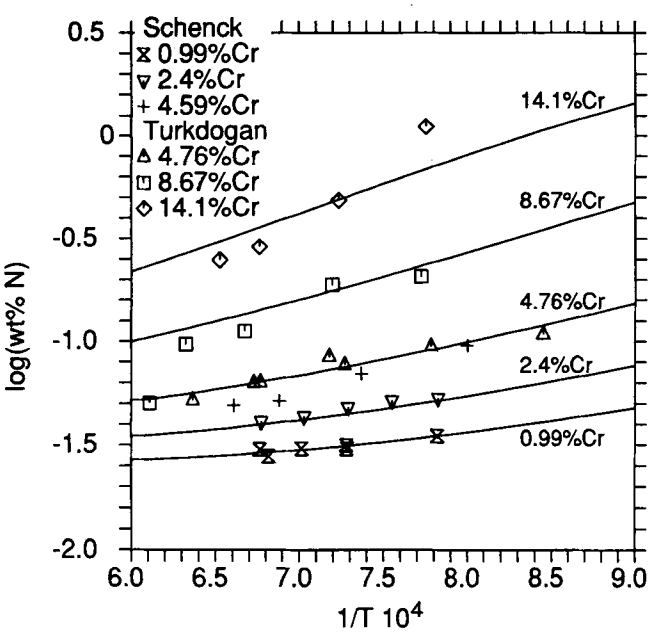

Fig. 5—The solubility of N in γ at different Cr contents and at 1 atm N_2 pressure together with experimental data.[19,22]

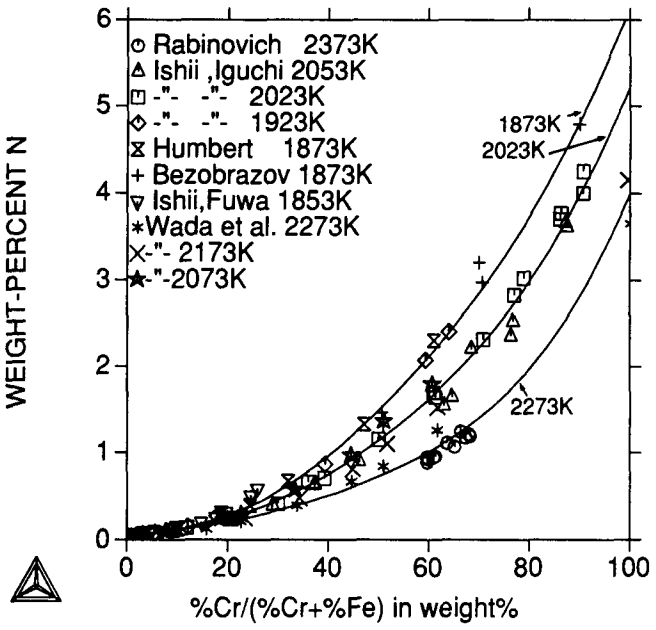

Fig. 6—The solubility of N in liquid Fe-Cr alloys in equilibrium with 1 atm N_2 gas. The solubility is calculated at three temperatures, 1873, 2023, and 2273 K, and experimental data from temperatures between 1853 and 2373 K[25-30] are plotted.

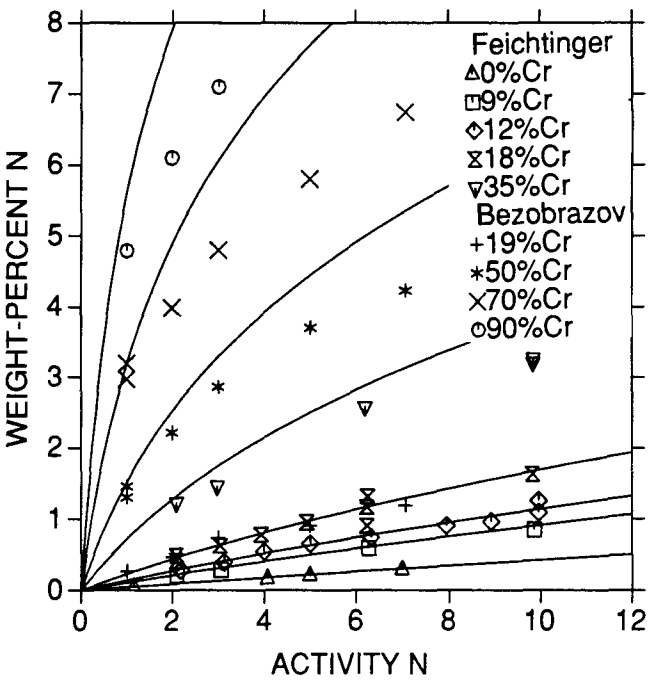

Fig. 8—The solubility of N in liquid Fe-Cr alloys at 1873 K.

samples with the highest Cr contents (70 and 90 pct Cr) would precipitate ε at 1873 K and the high N contents. The present description is in good agreement with the experimental data for alloys with up to 35 pct Cr for all N activities and up to 1 atm N_2 pressure for higher Cr contents.

IV. DISCUSSION

In the previous section, the results concerning single-phase α and γ and liquid were compared with experimental data. The optimized set of parameters (Table II) will now be used to recalculate all experimentally studied equilibria, and the agreement between calculated and experimental values will be discussed. The results of the present work are also compared with the previous assessment by Hertzman and Jarl.[2]

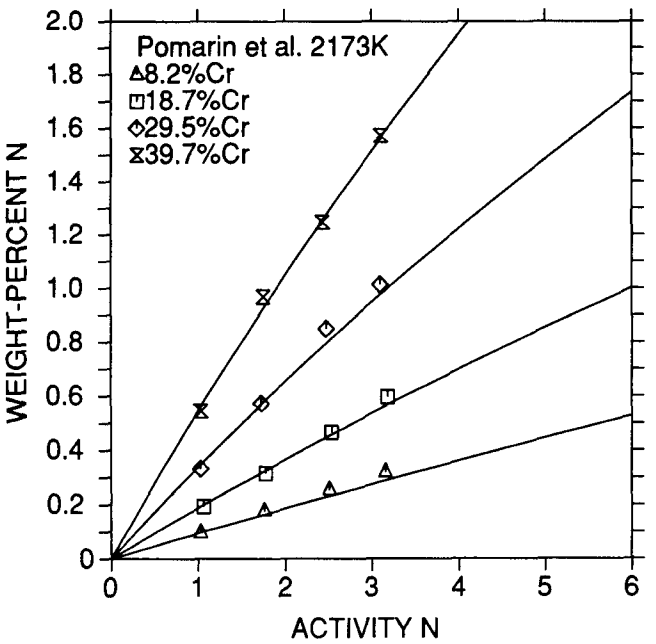

Fig. 7—The calculated solubility of N in liquid Fe-Cr alloys at 2173 K together with experimental data from Ref. 31.

The experimental data by Hertzman and Jarl[2] on the distribution of Cr between different phases are well described (Table III). The activity values (except the value 0.975 that was measured directly) were calculated by Hertzman and Jarl from the analyzed N content of the single-phase specimens contained in the same sealed capsule as the two- or three-phase equilibrium in question. The activity values were recalculated in the present work, using the set of parameters listed in Table II, giving values close to the previous results. In Figure 9, the calculated equilibria at 1273 K are compared with Hertzman and Jarl's data; the N activity is plotted *vs* the Cr content. The measured Cr content of each phase is represented by a symbol, and the two- and three-phase equilibria are connected by a dotted line (experimental tie line). The results of the present calculation are shown with a full line. The agreement is satisfactory for all equilibria. However, the CrN phase has a very small calculated solubility of Fe, although it has been measured to be 2 to 3 pct Fe. The results of the previous assessment[2] are shown in the same figure by dotted lines. The solubility limits of the ε phase are now improved, and the calculated activity for the $\gamma + \varepsilon +$ CrN equilibrium lies closer to the experimental value. The isothermal section at 1273 K is presented in Figure 10, together with experimental data by Imai *et al.*[23] and Hertzman and Jarl.[2] The agreement is very good, except for two single-phase γ data points that lie in the $\gamma +$ CrN region. Hertzman and Jarl[2] noted that this could be due to short annealing times. They found that the formation of CrN was slow. This figure also shows that Imai *et al.* found

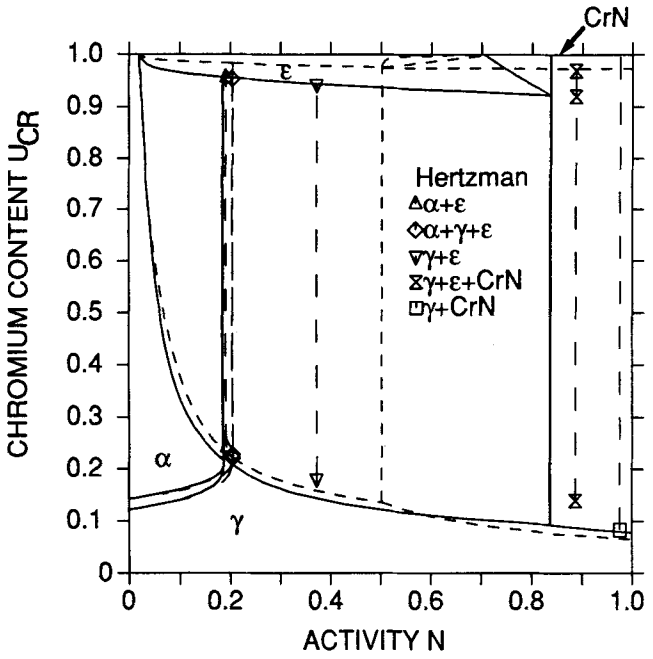

Fig. 9—Calculated equilibria in the Fe-Cr-N system at 1273 K together with experimental data by Hertzman and Jarl.[2] The calculation from the present work is shown by full lines, and the calculation by Hertzman and Jarl[2] is shown by dotted lines.

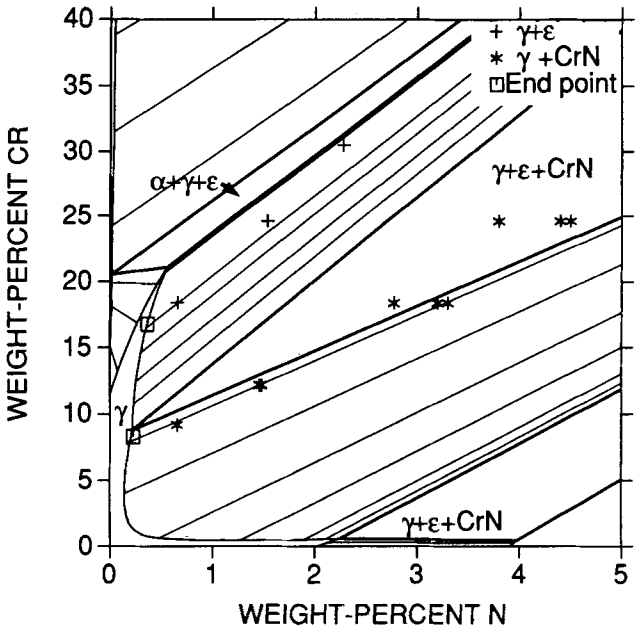

Fig. 11—The calculated isothermal section at 1273 K and experimental data from Ref. 2. The points marked "+" and "*" should lie on the same $\gamma + \varepsilon$ and γ + CrN tie line, respectively. The squares mark the end point of the tie lines and are plotted at the measured Cr content in γ and on the calculated γ phase boundary.

the $\alpha + \gamma + \varepsilon$ equilibrium at lower Cr contents than Hertzman and Jarl, but the present calculation fits the latter data. Hertzman and Jarl measured the N content by microprobe in several two-phase samples from the same capsule. They should lie on the same tie line. These data are compared with the present calculation in Figure 11, and the agreement is satisfactory.

The data by Jarl and Lindblad[7] on the distribution of Cr between different phases at 1473 K are also reproduced very well by the present calculation (Table IV). The calculation is compared with experimental data[7,14,15] in Figure 12, where the Cr content given as u_{Cr} is plotted *vs* the N activity, and the agreement is good. A part of the calculation by Hertzman and Jarl[2] is shown with dotted lines. The agreement on the γ/ε boundary has now been significantly improved. Figure 12 has been plotted up to $a_N = 5$, although there are no experimental data for high N activities. The plot shows that there is a $\gamma_1 + \gamma_2$ miscibility gap in this region. It has not been experimentally verified, but it was also present in Hertzman and Jarl's analysis but only at higher temperatures. Hertzman and Jarl showed that the miscibility gap causes a change in slope of the $\gamma/\gamma + \varepsilon$ phase boundary (Figures 10 and 13). The calculated 1473 K isothermal section is shown in Figure 13, together with experimental data.[7,14,15,23] Jarl and Lindblad measured the N activity, and not the N content, in their samples, so their data points were, in Figure 13, plotted at the N content calculated in the present work. Represented in this way, the data by Turkdogan and Ignatowicz[15] and Imai *et al.*[23] were not well fitted on the $\gamma/\alpha + \gamma$ side, since the activity data by Jarl and Lindblad were given a higher weight. However, as shown in Figure 12, activities measured by Jarl and Lindblad[7] and Turkdogan and Ignatowicz[15] are in quite good agreement and are well described by the calculation. Figures 3 and 4 show that the data by Turkdogan and Ignatowicz are well described in the α and γ one-phase regions. In Figure 14, the N activity *vs* the Cr content at 1513 K is plotted together with some experimental data by Sekita.[32] The agreement is very good, and it is seen that at this temperature, the $\gamma_1 + \gamma_2$ miscibility gap is no longer stable.

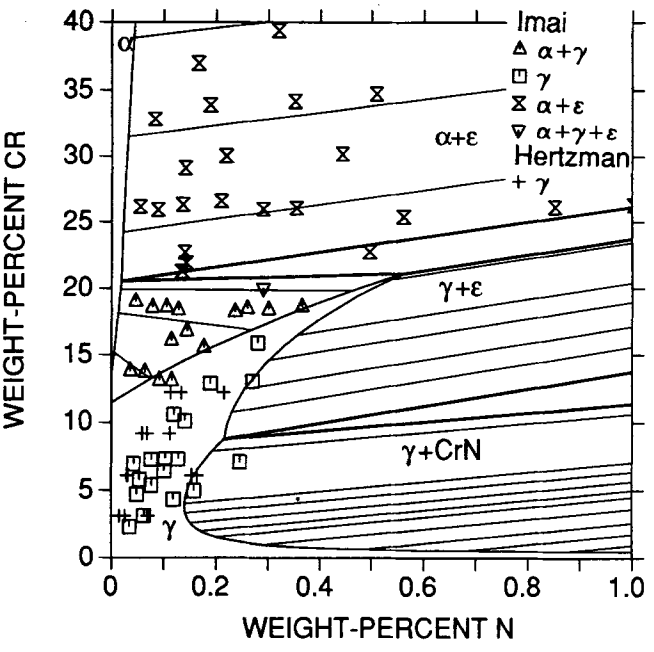

Fig. 10—The calculated isothermal section at 1273 K and experimental data from Refs. 2 and 23.

Imai *et al.*[23] studied the Cr-Fe-N system at temperatures between 973 and 1573 K. It was shown above

Table IV. Distribution of Chromium among α, γ, and ε at 1473 K*

Phases	a_N	Ferrite (α) u^{α}_{Cr}	Austenite (γ) u^{γ}_{Cr}	ε (Cr_2N) u^{ε}_{Cr}	
$\alpha + \gamma$	0.74	0.188	0.185	—	exp.
	0.77	0.188	0.183	—	calc.
$\alpha + \gamma$	0.74	0.224	0.243	—	exp.
	0.76	0.224	0.235	—	calc.
$\alpha + \gamma$	0.76	0.253	0.276	—	exp.
	0.71	0.253	0.279	—	calc.
$\alpha + \gamma$	0.62	0.162	0.152	—	exp.
	0.69	0.162	0.151	—	calc.
$\alpha + \gamma$	0.62	0.297	0.325	—	exp.
	0.64	0.297	0.335	—	calc.
$\gamma + \varepsilon$	0.97	—	0.360	0.905	exp.
	0.84	—	0.360	0.905	calc.
$\alpha + \gamma + \varepsilon$	—	0.346	0.393	0.899	exp.
	0.58	0.342	0.379	0.913	calc.

*Values calculated in the present work (noted "calc." in the last column) are compared with experimental data from the work by Jarl and Lindblad[7] (noted "exp." in the last column).

(Figures 10 and 13) that the present calculation is in satisfactory agreement with data at 1273 and 1473 K. At 1573 K (Figure 15), the calculated solubility of N in α and γ in equilibrium is larger than indicated by the experimental data. However, the calculated solubility in α is slightly too low compared with the experimental data at 1373 K shown in Figure 16. The solubility in γ in equilibrium with α is too high for all temperatures above 1323 K. As discussed above, this is due to the higher weighting of the data by Hertzman and Jarl[2] and Jarl and Lindblad.[7] For the same reason, the calculated Cr content of the $\alpha + \gamma + \varepsilon$ equilibrium lies higher than measured by Imai *et al.*[23] at temperatures below 1323 K. At 1173 K, the calculated γ-phase region is less wide than measured by Imai *et al.* This could be due to short annealing times, as discussed above for the section at 1273 K. It is worth noting that Imai *et al.* never reported any CrN phase. The isothermal section at 973 K was also studied by Firrao *et al.*[6,24] (Figure 17). Imai *et al.*

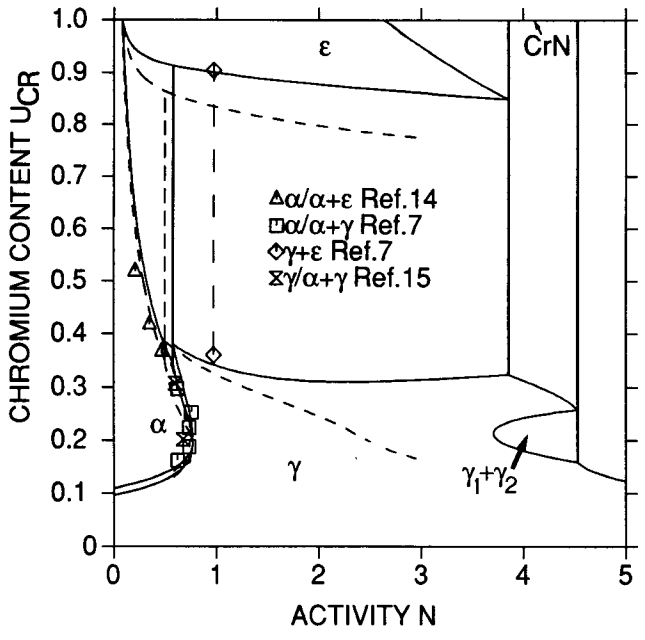

Fig. 12—Calculated equilibria in the Fe-Cr-N system at 1473 K together with experimental data by Jarl and Lindblad,[7] Schwerdtfeger,[14] and Turkdogan and Ignatowicz.[15] The calculation from the present work is shown by full lines, and the calculation by Hertzman and Jarl[2] is shown by dotted lines.

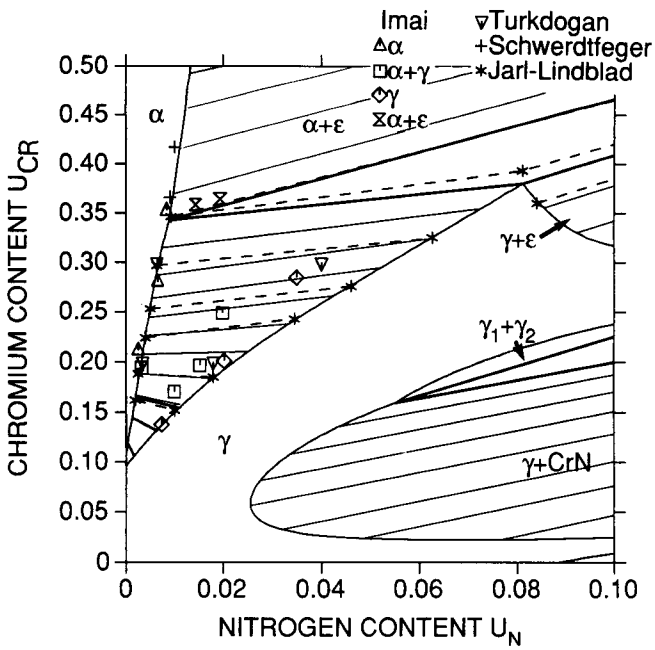

Fig. 13—The calculated isothermal section at 1473 K together with experimental data from Refs. 7, 14, 15, and 23. The experimental data points by Jarl and Lindblad[7] were plotted at the N content calculated in the present work.

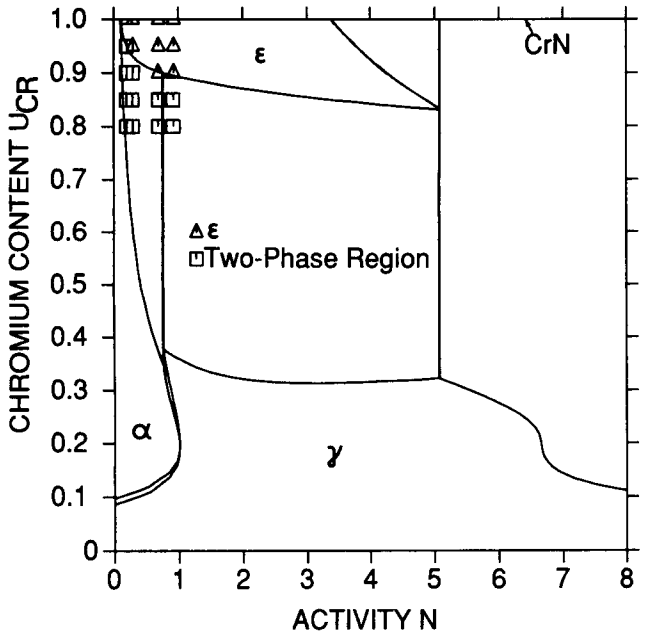

Fig. 14—Experimental[32] and calculated equilibria at 1513 K.

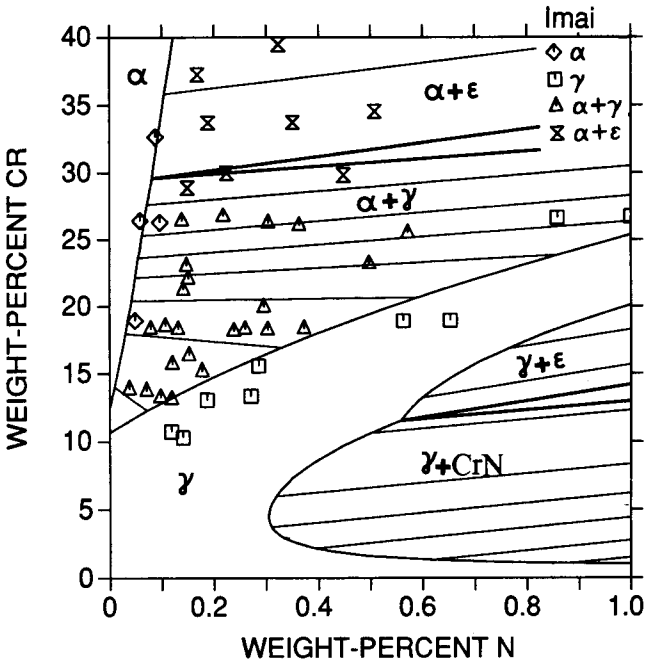

Fig. 16—The calculated isothermal section at 1373 K together with experimental data from Ref. 23.

found the three-phase region α + CrN + Fe_4N, whereas Firrao *et al.* found α + γ + CrN. The present calculation agrees with the latter. In Figure 17, a number of single-phase ε data points lie in the ε + CrN region. Firrao *et al.* found that the Fe-rich ε phase can dissolve 20 pct Cr, a result which was impossible to reproduce. The agreement is otherwise good.

Figure 18 shows the calculated projection of the liquidus surface and the four phase planes for the invariant equilibria involving the liquid. It should be noted that the extrapolation of the liquid to high N contents is uncertain, because all experimental data concern low N contents. The only study of the liquidus surface is by Okamoto and Naito.[33] However, Imai *et al.*[23] found results inconsistent with those of Okamoto and Naito and could show that this was due to the fact that Okamoto and Naito included a nonequilibrium Cr_2N phase in their equilibrium diagrams. Imai *et al.* estimated that an $L + \alpha \rightarrow \gamma + \varepsilon$ reaction should lie at about 1600 K and that the compositions of the α and γ phases should be about 39 pct Cr and 0.25 pct N and 35 pct Cr and 1.3 pct N, respectively. These compositions are in good agreement with the present work but very far from the results by Okamoto and Naito.

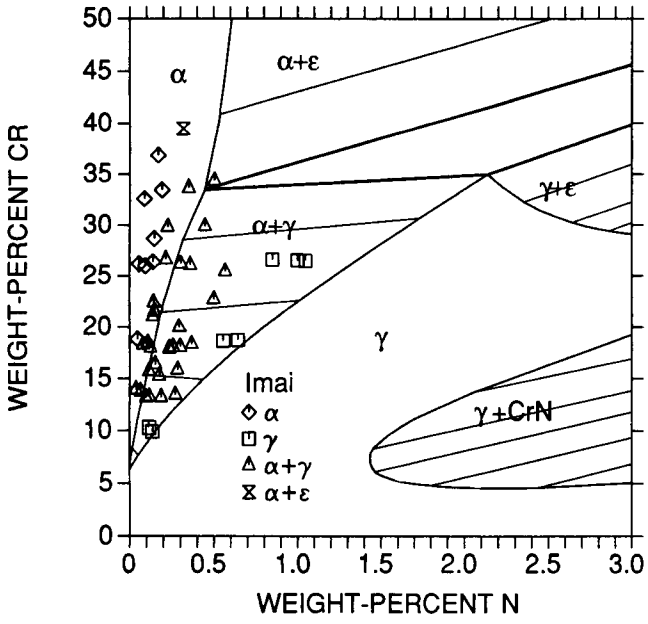

Fig. 15—The calculated isothermal section at 1573 K together with experimental data from Ref. 23.

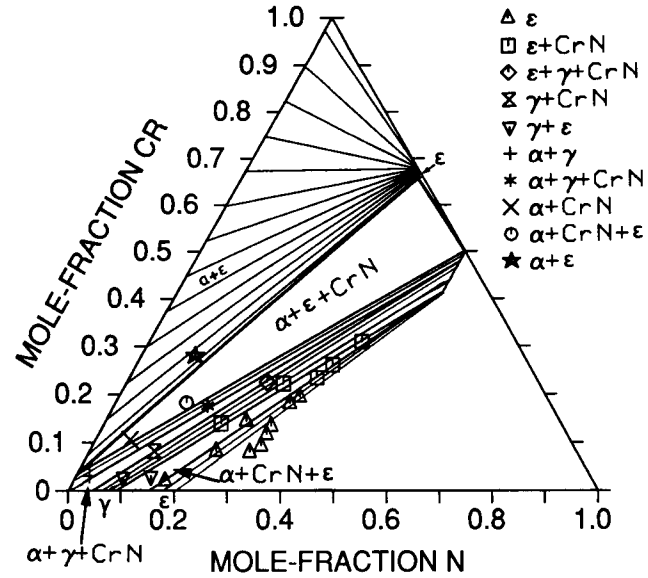

Fig. 17—The calculated isothermal section at 973 K together with experimental data from Ref. 6.

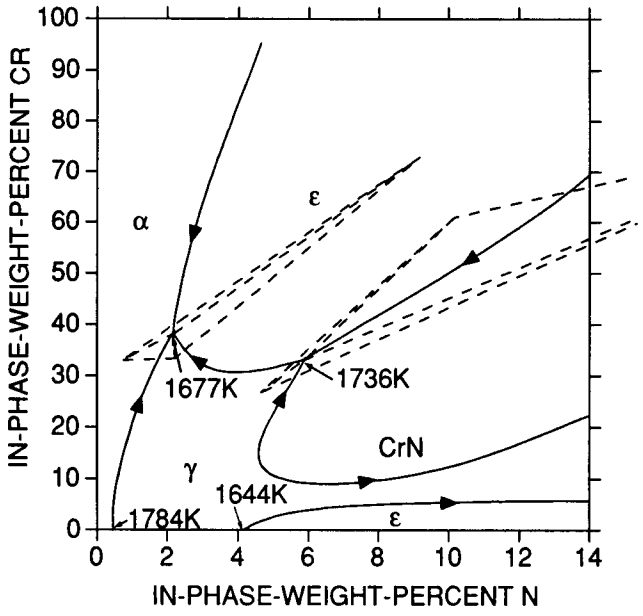

Fig. 18—The calculated projection of the liquidus surface. The four phase planes are shown with dashed lines.

V. SUMMARY

An analysis of the thermodynamic properties of the Cr-Fe-N system is presented. A set of parameters describing the Gibbs energy of each phase is given, which permits calculation of all types of phase equilibria and their comparison with experimental data. In most cases, the agreement is good. The analysis shows that there are some differences in the experimental results on locations of phase boundaries between Imai *et al.*[23] and Jarl and Lindblad.[7] The present work fits the latter. Compared to a previous assessment, recent experimental data have been used as well as the older data, and the liquid phase was now included in the assessment. For some equilibria, the agreement is now better than in the previous assessment. A good fit was obtained for the liquid phase at low N contents. However, the extrapolations of the liquid phase to high N contents are uncertain.

ACKNOWLEDGMENTS

I would like to thank Professor Mats Hillert for advice, constructive criticism, and the help received during the preparation of this paper. This work was financially supported by The Swedish Steel Producers Association.

REFERENCES

1. V. Raghavan: *Trans. Indian Inst. Met.*, 1984, vol. 37, pp. 671-89.
2. S. Hertzman and M. Jarl: *Metall. Trans. A*, 1987, vol. 18A, pp. 1745-52.
3. J.-O. Andersson and B. Sundman: *CALPHAD*, 1987, vol. 11, pp. 83-92.
4. K. Frisk: Trita-Mac-0393, Royal Institute of Technology, Stockholm, Sweden, Apr. 1989.
5. H. Feichtinger, A. Satir-Kolorz, and Z. Xiao-Hong: *HNS 88*, Int. Conf. on High-Nitrogen Steels, Lille, France, Institute of Metals, London, England, 1989.
6. D. Firrao, M. Rosso, and B. de Benedetti: *Atti. Accad. Sci. Torino*, 1980, vol. 114, pp. 383-93.
7. M. Jarl and B. Lindblad: *Metall. Trans. A*, 1978, vol. 9A, pp. 1891-92.
8. M. Hillert and L.-I. Staffansson: *Acta Chem. Scand.*, 1970, vol. 24, pp. 3618-26.
9. J.-O. Andersson: *Int. J. Thermophys.*, 1986, vol. 6, pp. 411-19.
10. J.-O. Andersson, A. Fernández Guillermet, and P. Gustafson: Trita-Mac-0319, Royal Institute of Technology, Stockholm, Sweden, Oct. 1986.
11. A. Fernández Guillermet and P. Gustafson: *High Temp.-High Pressures*, 1985, vol. 16, pp. 591-610.
12. M. Hillert and M. Jarl: *CALPHAD*, 1978, vol. 2, pp. 227-38.
13. B. Jansson: Ph.D. Thesis, Royal Institute of Technology, Stockholm, Sweden, 1984.
14. K. Schwerdtfeger: *Z. Metallkd.*, 1975, vol. 66, pp. 139-43.
15. E.T. Turkdogan and S. Ignatowicz: in *Physical Chemistry of Process Metallurgy, Part 1*, G.R. St. Pierre, ed., Interscience Publishers, New York, NY, 1961, pp. 617-32.
16. M. Lebienvenu and B. Dubois: *Ann. Chim. Fr.*, 1985, vol. 10, pp. 639-44.
17. H. Zitter and L. Habel: *Arch. Eisenhüttenwes.*, 1973, vol. 44, pp. 181-88.
18. T. Mori, R.K. Shinmyo, E. Ichise, and S. Koyama: *Mem. Fac. Eng. Kyoto Univ.*, 1963, vol. 25, pp. 175-87.
19. E.T. Turkdogan and S. Ignatowicz: *JISI*, 1958, vol. 188, pp. 242-47.
20. M. Lebienvenu and B. Dubois: *Ann. Chim. Fr.*, 1983, vol. 8, pp. 423-33.
21. H.J. Grabke, S.K. Iyer, and S.R. Srinivasan: *Z. Metallkd.*, 1975, vol. 66, pp. 286-92.
22. H. Schenck, M.G. Frohberg, and F. Reinders: *Stahl Eisen*, 1963, vol. 83, pp. 93-99.
23. Y. Imai, T. Masumoto, and K. Maeda: *Sci. Rep. Res. Inst. Tohoku Univ., A*, 1967, vol. 19, pp. 35-49.
24. D. Firrao, M. Rosso, and B. de Benedetti: *Atti. Accad. Sci. Torino*, 1980, vol. 114, pp. 423-31.
25. J.C. Humbert and J.F. Elliott: *Trans. TMS-AIME*, 1960, vol. 218, pp. 1076-88.
26. H. Wada, K. Gunji, and T. Wada: *Trans. ISIJ*, 1968, vol. 8, pp. 329-36.
27. S.V. Bezobrazov, A.G. Ponomarenko, and E.N. Inozemtseva: *Russ. Metall.*, 1980, vol. 3, pp. 42-48.
28. F. Ishii and T. Fuwa: *Tetsu-to-Hagané*, 1982, vol. 68, pp. 1560-68.
29. F. Ishii, Y. Iguchi, and S. Ban-Ya: *Tetsu-to-Hagané*, 1983, vol. 69, pp. 913-20.
30. A.V. Rabinovich, G.M. Grigorenko, V.V. Yaroshenko, Y.M. Pomarin, and M.I. Taras'ev: *Probl. Spets. Elektrometall.*, 1985, vol. 1, pp. 63-66.
31. Y.M. Pomarin, G.M. Grigorenko, Y.V. Latash, and S.A. Kanibolotskii: *Russ. Metall. (Metally)*, 1984, vol. 6, pp. 7-11.
32. Takashi Sekita: Master of Engineering Thesis, Tokyo Institute of Technology, Tokyo, Japan, 1975.
33. M. Okamoto and T. Naito: *Tetsu-to-Hagané*, 1963, vol. 49, pp. 1915-21.